BBA - Biomembranes 1860 (2018) 1793–1802

Contents lists available at ScienceDirect

BBA - Biomembranes

journal homepage: www.elsevier.com/locate/bbamem

A blend of two resveratrol derivatives abolishes hIAPP amyloid growth and membrane damage☆

Michele F.M. Sciacca[a], Rosa Chillemi[b], Sebastiano Sciuto[b], Valentina Greco[b], Concetta Messineo[b], Samuel A. Kotler[c], Dong-Kuk Lee[d], Jeffrey R. Brender[c], Ayyalusamy Ramamoorthy[c], Carmelo La Rosa[b,*], Danilo Milardi[a,*]

[a] Istituto CNR di Biostrutture e Bioimmagini- Sede Secondaria di Catania, Via Paolo Gaifami 18, 95126 Catania, Italy
[b] Università degli Studi di Catania, Dipartimento di Scienze Chimiche, Viale Andrea Doria 6, 95125 Catania, Italy
[c] Biophysics and Department of Chemistry, University of Michigan, Ann Arbor, MI 48109-1055, USA
[d] Department of Fine Chemistry, Seoul National University of Science and Technology, Seoul 01811, Republic of Korea

ARTICLE INFO

Keywords:
Cytoxicity
Protection
Natural compounds
Oxydative stress
Aggregation

ABSTRACT

Type II diabetes mellitus (T2DM) is characterized by the presence of amyloid deposits of the human islet amyloid polypeptide (hIAPP) in pancreatic β-cells. A wealth of data supports the hypothesis that hIAPP's toxicity is related to an abnormal interaction of amyloids with islet cell membranes. Thus, many studies aimed at finding effective therapies for T2DM focus on the design of molecules that are able to inhibit hIAPP's amyloid growth and the related membrane damage as well. Based on this view and inspired by its known anti-amyloid properties, we have functionalized resveratrol with a phosphoryl moiety (4′-*O*-PR) that improves its solubility and pharmacological properties. A second resveratrol derivative has also been obtained by conjugating resveratrol with a dimyristoylphosphatidyl moiety (4′-DMPR). The use of both compounds resulted in abolishing both amyloid growth and amyloid mediated POPC/POPS membrane damage in tube tests. We propose that a mixture of a water-soluble anti-aggregating compound and its lipid-anchored derivative may be employed as a general strategy to prevent and/or to halt amyloid–related membrane damage.

1. Introduction

Diabetes mellitus type II (T2DM) is one of the most common degenerative and disabling pathologies for the aged people in developed countries [1–3]. T2DM is a member of a class of pathologies named Protein Conformational Diseases (PCD) characterized by the presence of protein aggregates rich in β-sheet structure, known as amyloid fibrils [4]. The cytotoxic mechanisms of amyloidogenic proteins on their target cells are subject of intense debate. However, it is widely known that proteotoxic effects are irreversible and frequently cell functionality is completely lost well before amyloid fibers are detectable.

The protein involved in the development of T2DM is the human Islet Amyloid Polypeptide (hIAPP), also known as Amylin [5–7]. HIAPP, in its monomeric form, is an unstructured C-terminally amidated 37-residues peptide co-secreted with insulin in pancreatic Langerhans' β-cells. Amino acid sequences of IAPP peptide is given in Fig. 1. In patients affected by T2DM, hIAPP aggregates into amyloid fibers detectable in the extracellular space of the pancreas. Although a close relationship between hIAPP amyloid growth and T2DM is largely accepted, the lack of complete knowledge about the factors involved on the onset of the disease has hampered to date the development of effective drugs. Substantial evidence points to an abnormal interaction of oligomeric forms of hIAPP with cell membranes as the prevalent cause of toxicity [8]. A number of papers have suggested, in particular, that small sized amyloid assemblies may penetrate and damage the cell membrane by forming ion permeable pores [9–17]. By contrast, other reports have evidenced that membrane disruption may also occur via a "detergent-like" mechanism as a consequence of the growth of amyloid fibrils on the membrane surface [18]. Some of us have recently reported that, in hIAPP-mediated membrane damage, both these mechanisms can occur [19,20]. In the first step, the protein as monomer or small-sized oligomer interacts with the membrane leading to the formation of non-selective pores. The second step, which occurs later, is associated with the growth of fibers on the surface of the membrane and leads to the complete fragmentation of the membrane through amyloid-assisted lipid extraction (micellization). This evidence implies that a molecule

☆ This article is part of a Special Issue entitled: Protein Aggregation and Misfolding at the Cell Membrane Interface edited by Ayyalusamy Ramamoorthy.

* Corresponding authors.
E-mail addresses: clarosa@unict.it (C. La Rosa), dmilardi@unict.it (D. Milardi).

https://doi.org/10.1016/j.bbamem.2018.03.012
Received 5 December 2017; Received in revised form 31 January 2018; Accepted 13 March 2018
Available online 17 March 2018
0005-2736/ © 2018 Elsevier B.V. All rights reserved.

Table 1
Kinetic parameters of ThT traces relative to hIAPP fiber growth in the presence of LUVs and resveratrol/4′-*O*-PR/4′-DMPR. Curves were fitted by using Eq. (1). Lag time (t_{lag}) was calculated by using Eq. (2). All parameters are reported as average ± s.d. calculated from 3 independent measurements.

Sample	ThT_{max} (A.U.)	$t_{1/2}$ (min)	t_{lag} (min)	k (min^{-1})
hIAPP	2.03 ± 0.02	402.1 ± 2.2	388.5 ± 2.2	0.035 ± 0.002
hIAPP 7:3 POPC/POPS	2.02 ± 0.015	310.5 ± 3.1	289.6 ± 3.1	0.024 ± 0.002
hIAPP 7:3 POPC/POPS Resveratrol 1.25 μM	1.68 ± 0.03	319.6 ± 4.0	307.1 ± 4.0	0.041 ± 0.003
hIAPP 7:3 POPC/POPS Resveratrol 2.5 μM	2.12 ± 0.01	274.4 ± 1.8	254.4 ± 1.8	0.025 ± 0.001
hIAPP 7:3 POPC/POPS Resveratrol 5 μM	1.82 ± 0.02	343.2 ± 2.1	320.4 ± 2.1	0.022 ± 0.002
hIAPP 7:3 POPC/POPS 4′-*O*-PR 1.25 μM	1.14 ± 0.04	276.3 ± 4.2	260.1 ± 4.2	0.031 ± 0.004
hIAPP 7:3 POPC/POPS 4′-*O*-PR 2.5 μM	1.15 ± 0.03	292.9 ± 4.0	279.4 ± 4.0	0.037 ± 0.005
hIAPP 7:3 POPC/POPS 4′-*O*-PR 5 μM	1.10 ± 0.05	315.3 ± 4.5	294.8 ± 4.5	0.024 ± 0.007
hIAPP 7:3 POPC/POPS/4′-DMPR 1.25 μM	1.58 ± 0.025	337.1 ± 4.2	301.5 ± 4.2	0.014 ± 0.002
hIAPP 7:3 POPC/POPS/4′-DMPR 2.5 μM	1.10 ± 0.03	291.8 ± 4.4	258.4 ± 4.4	0.015 ± 0.003
hIAPP 7:3 POPC/POPS/4′-DMPR 5 μM	n.d	n.d.	n.d.	n.d.

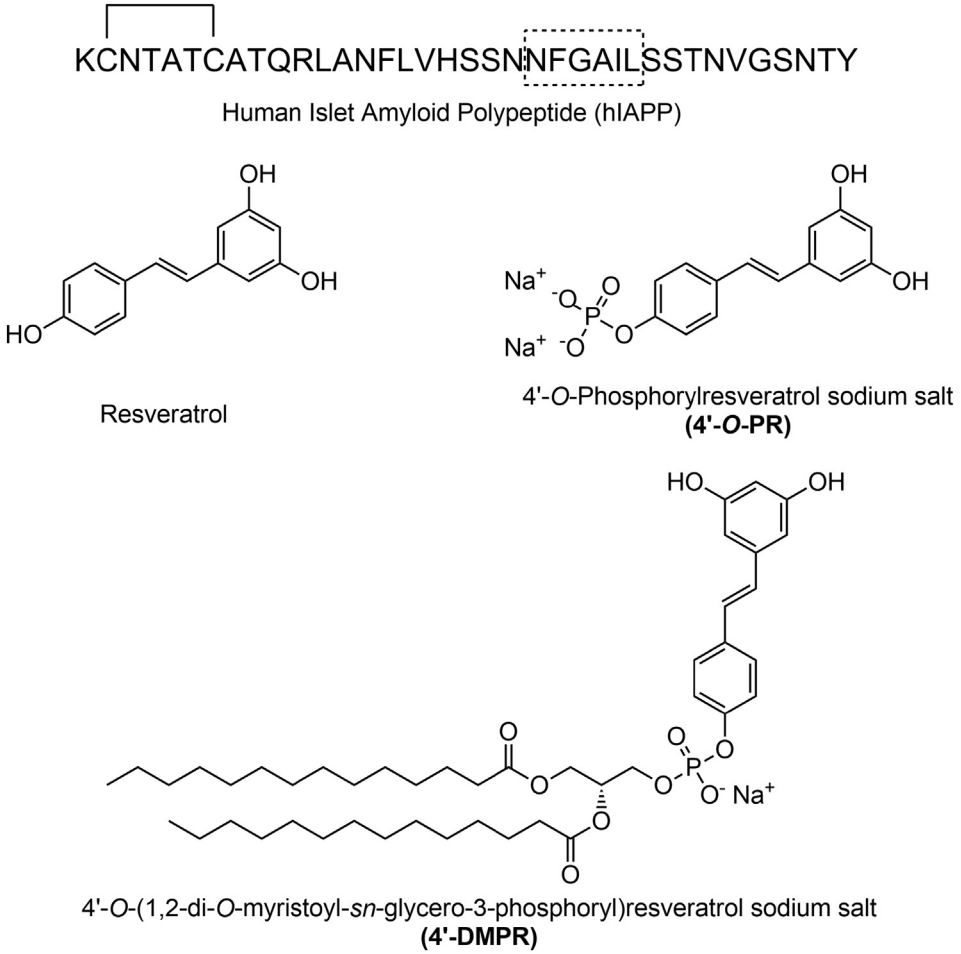

Fig. 1. Primary sequence of hIAPP. The amyloidogenic region is evidenced by a dashed box. Chemical structures of resveratrol and its two derivatives 4′-*O*-PR and 4′-DMPR investigated in this study.

designed to block fibril growth can work as a protective agent against amyloid toxicity and shift the target of research towards the development of molecules that can prevent both pore formation and fiber growth. The use of amyloid inhibitors such as curcumin [21], silybin [22], green tea extracts [23] and other natural compounds [24–26] due also to their low toxicity and high availability is of growing interest in this field. In particular resveratrol, a natural component of red wine with many pharmacological properties, is vastly studied [27–30]. Previous biophysical studies have shown that resveratrol, despite its poor water solubility (3 mg/100 mL) [31], is a promising inhibitor of fiber growth of some of the amyloidogenic proteins [32]. Based on these premises, we designed and synthesized two distinct resveratrol derivatives (Fig. 1). The presence of the phosphoryl moiety in the first compound, 4′-*O*-phosphorylresveratrol (4′-*O*-PR), is thought to increase

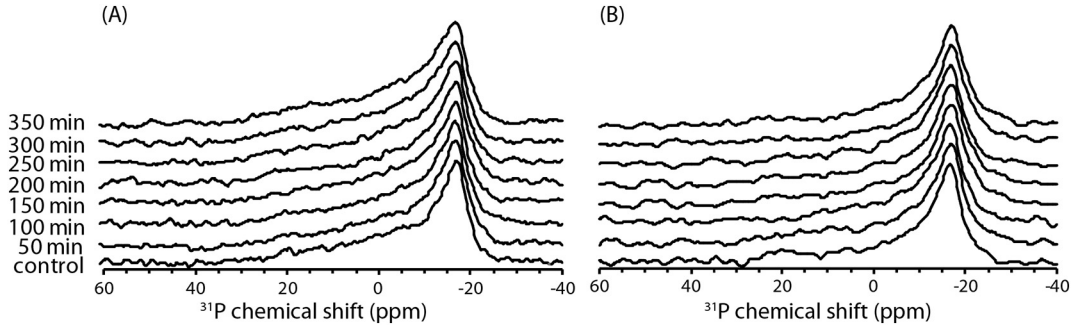

Fig. 2. Static ^{31}P NMR spectra of 7:3 POPC/POPS LUVs treated with (A) 1 mol% hIAPP or (B) 3 mol% hIAPP as a function of time. ^{31}P NMR spectra initially were collected prior to adding hIAPP (bottom). Each subsequent spectrum was collected after every 50 min. The lack of an isotropic peak ~0 ppm indicates hIAPP does not induce small, isotropically tumbling membrane fragments. Experiments were performed at 37 °C in 10 mM HEPES, 100 mM NaCl, pH 7.4.

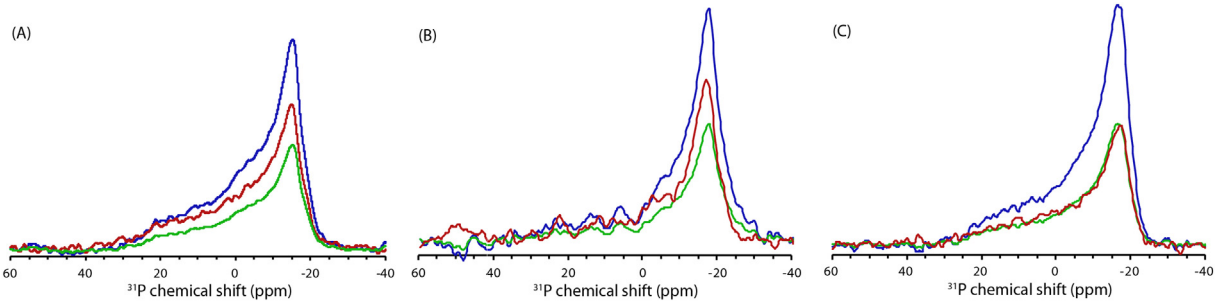

Fig. 3. Static ^{31}P NMR spectra of 7:3 POPC/POPS LUVs in the absence of peptide (A), with 1 mol% hIAPP (B), and with 3 mol% hIAPP (C) at 10 h of incubation (blue spectra). Spectra of LUVs after the inclusion of paramagnetic Mn^{2+} ions (red spectra). The green spectra indicate half of the calculated intensity measured prior to the addition of Mn^{2+} ions. Experiments were performed at 37 °C in 100 mM NaCl, 10 mM HEPES, pH 7.4. NMR results showed a threshold hIAPP concentration below which no pore formation was detected. Thus, further investigations were carried out using protein concentration of 3% higher than lipid membranes.

the solubility of resveratrol retaining its anti-aggregation properties. In the second compound, 4′-*O*-(1,2-di-*O*-myristoyl-sn-glycero-3-phosphoryl resveratrol (4′-DMPR), the presence of the lipid tail is thought to anchor the resveratrol functional group on the membrane surface preventing the fiber-dependent membrane disruption process. In this study we performed dye-leakage, ^{31}P solid state NMR, and ThT experiments to test the ability of 4′-*O*-PR to stabilize monomeric species of hIAPP in solution thus preventing poration of POPC/POPS model membranes. Parallel experiments were performed with model membranes which incorporate 4′-DMPR to verify if this compound can halt lipid extraction and membrane disruption induced by hIAPP amyloid growth. We also tested the synergistic effect of a mixture of the two derivatives which completely inhibits both steps of membrane disruption.

2. Materials and methods

2.1. Materials

hIAPP was purchased from Bachem (Bubendorf, Switzerland) with a purity > 98%. 1-Palmitoyl-2-oleoyl-*sn*-glycero-3-phosphocholine (POPC) and 1-palmitoyl-2-oleoyl-*sn*-glycero-3-phospho-L-serine sodium salt (POPS) were purchased from Avanti Polar lipids Inc. (Alabaster, AL). 6-Carboxyfluorescein, Thioflavin T (ThT), 1,1,1,3,3,3-hexafluoro-2-propanol (HFIP) and all other salts were purchased from Sigma-Aldrich (St. Louis, MO) with a purity of 99%. Resveratrol was purchased from Sigma-Aldrich (St. Louis, MO). 4′-*O*-Phosphorylresveratrol (4′-*O*-PR) and 4′-*O*-(1,2-di-*O*-myristoyl-*sn*-glycero-3-phosphoryl) resveratrol (4′-DMPR) were synthesized in our labs as previously described [33,34].

2.2. Preparation of model membranes

In this study, we used large unilamellar vesicles (LUVs) composed of 7:3 POPC/POPS in molar ratio. Model membranes were prepared as described elsewhere [10]. Briefly, aliquots of lipid stock solutions in chloroform were dried by using a stream of dry nitrogen and evaporated under high vacuum to dryness in a round-bottomed flask. Multilamellar vesicles (MLVs) were obtained by hydrating the lipid film with an appropriate amount of phosphate buffer (10 mM buffer, 100 mM NaCl, pH 7.4) and dispersing by vigorous stirring in a water bath. LUVs were obtained by extruding MLVs through polycarbonate filters (pore size = 100 nm, Nuclepore, Pleasanton, CA) mounted in a mini-extruder (Avestin, Ottawa, Canada) fitted with two 0.5 mL Hamilton gastight syringes (Hamilton, Reno, NV). Samples were typically subjected to 23 passes through two filters in tandem and as recommended elsewhere [35].

2.3. Human-IAPP preparation

To prevent the presence of any preformed aggregates, hIAPP was initially dissolved in HFIP at a concentration of 1 mg/mL and then lyophilized overnight. To be used for the experiments, the lyophilized powder was initially dissolved in DMSO to obtain a stock solution with a final concentration of 250 μM. Each stock solution of hIAPP was used immediately after preparation.

2.4. ThT measurements

Kinetics of amyloid formation was measured using the well-known Thioflavin T (ThT) assay. Samples were prepared by adding 1 μL of the 250 μM DMSO peptide stock solution to 100 μL of 25 μM LUV solution (in 10 mM phosphate buffer pH 7.4, 100 mM NaCl, containing 10 μM ThT) and by adding the required amount of resveratrol or resveratrol derivatives. Experiments were carried out in Corning 96 well non-binding surface plates. Time traces were recorded using a Varioskan (ThermoFisher, Walham, MA) plate reader using a λ_{ecc} of 440 nm and a

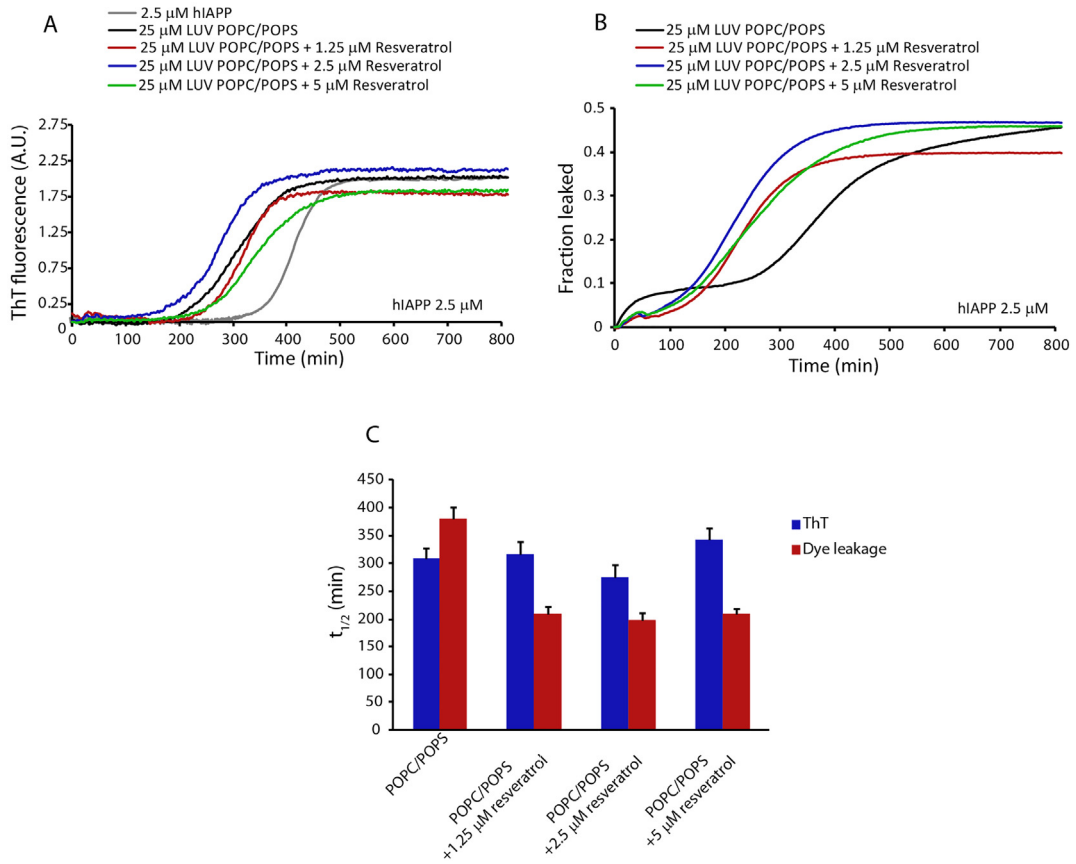

Fig. 4. A) Effect of resveratrol (1.25–5.0 μM) on hIAPP fiber formation kinetics and membrane disruption in the presence of 25 μM 7:3 POPC/POPS LUVs. HIAPP concentration was 2.5 μM. All measurements were performed in 10 mM phosphate buffer, 100 mM NaCl, pH 7.4 at 25 °C. Fiber growth kinetics of lipid-free hIAPP is also reported for comparison (grey curve). The traces shown are the average of 3 independent experiments. B) Effect of resveratrol on the mechanism of 7:3 POPC/POPS LUV disruption induced by hIAPP measured by dye leakage assay. All measurements were performed in 10 mM phosphate buffer, 100 mM NaCl, pH 7.4 at 25 °C. The curves shown are the average of 3 independent experiments. C) Comparison of $t_{1/2}$ of fiber formation and membrane damage processes (see also Table 1).

Table 2
Molecular descriptors of resveratrol and 4′-*O*-PR.

Molecular descriptors	Resveratrol	4′-*O*-PR
MW	228.25	306.21
HBD	3	2
HBA	3	6
Log P	2.99	−1.01
TPSA	60.68	112.88
nrotb	2	4

Acronyms: MW = molecular weight; HBD = number of hydrogen bond donor groups; HBA = number of hydrogen bond acceptors; Log P = logarithm of the partition coefficient octanol/water; TPSA = Total polar surface area; nrotb = number of rotatable bonds.

λ_{em} of 485 nm at 25 °C, shaking the samples for 10 s before each read. All ThT curves represent the average of three independent experiments with each run in quadruplicate. To obtain the kinetics parameters relative to the ThT assay we fitted the data obtained by three independent measurements with the equation:

$$ThT\ fluorescence = \frac{ThT_{max}}{1 + e^{-k(t-t_{1/2})}} \quad (1)$$

In this equation ThT_{max} is the maximum value of the ThT signal, which is qualitatively correlated with the amount of fiber formed; $t_{1/2}$ is the time to half which is defined as the time the signal needs to reach 50% of the maximum; k is the apparent fiber growth rate. We also calculated the lag time (t_{lag}), which is the time the signal needs to reach 10% of the maximum, and is considered the starting point of fiber formation, by using the equation:

$$t_{lag} = t_{1/2} - \left(\frac{1}{2k}\right) \quad (2)$$

2.5. Membrane leakage experiments

Membrane leakage experiments were performed by measuring the leakage of 6-carboxyfluorescein dye from LUVs. Dye-filled LUVs were prepared by hydrating the dry lipid film with the buffer solution containing 6-carboxyfluorescein (70 mM 6-carboxyfluorescein, pH 7.4) according to the procedure described above. To remove non encapsulated 6-carboxyfluorescein we placed the solution containing LUVs on a Sephadex G50 gel exclusion column (Sigma-Aldrich, St.Louis, MO) and eluted using the buffer solution. The final concentration of lipids was checked by using the Stewart assay as described elsewhere [36]. Membrane damage was quantified by the increase in fluorescence emission intensity of 6-carboxyfluorescein due to its dilution (dequenching) in buffer as a consequence of the membrane leakage. All dye leakage curves represent the average ± s.d. calculated from three independent experiments with each run in quadruplicate. Kinetics of dye-leakage were evaluated by calculating the $t_{1/2}$.

2.6. Determination of micelle formation

We detected the presence of micelles (here operationally defined as the ensemble of lipids detached from LUVs due to fibril induced membrane disruption) as described elsewhere [37]. We measured the

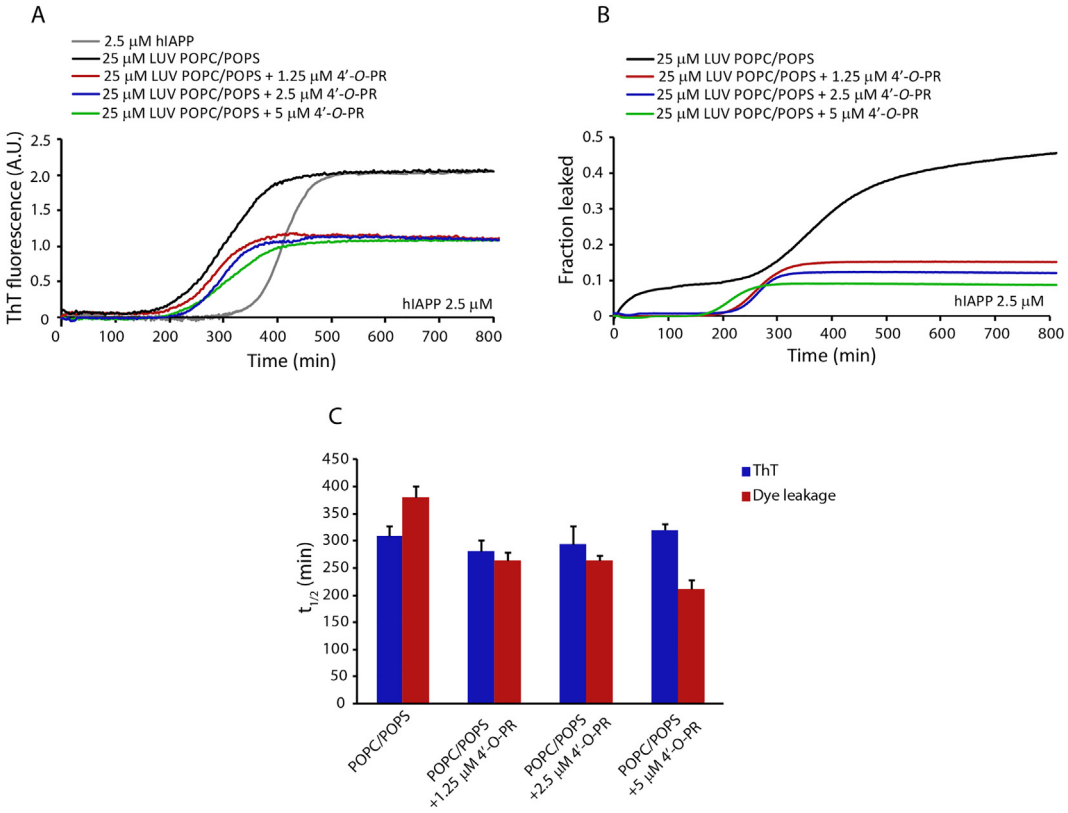

Fig. 5. A) Effect of 4′-*O*-PR on the kinetics of hIAPP fiber formation in the presence of 7:3 POPC/POPS LUVs measured by ThT assay. All measurements were performed in 10 mM phosphate buffer, 100 mM NaCl, pH 7.4 at 25 °C. Fiber growth kinetics of lipid-free hIAPP is also reported for comparison (grey curve). The curves shown are the average of 3 experiments. B) Effect of 4′-*O*-PR on hIAPP-induced disruption of 7:3 POPC/POPS LUVs measured dye leakage assay. All measurements were performed in 10 mM phosphate buffer, 100 mM NaCl, pH 7.4, at 25 °C. The traces shown are the average of 3 experiments. C) Comparison of $t_{1/2}$ of fiber formation and the second step of membrane disruption in the presence of increasing amounts of 4′-*O*-PR (see also Table 1).

lipid concentration in the supernatant after centrifugation of the 100 nm LUVs. Solutions of 7:3 POPC/POPS at a final concentration of 1 mg/mL were prepared as described above, except that the solutions were extruded through 100 nm membranes. We first incubated 2.5 μM hIAPP with 250 μL of the LUV solution for 1 day to allow the formation of amyloid fibers. After incubation with hIAPP, the samples were centrifuged for 40 min at 14,000 rpm, and the supernatant, which contained any resulting micelles, was collected, diluted in 1 mL of chloroform, and analyzed in terms of lipid concentration. Solutions without hIAPP were set as controls. Lipid concentrations in the supernatant were detected via the Stewart assay as described elsewhere [38].

2.7. Sample preparation for ^{31}P NMR experiments

LUVs for NMR experiments were prepared as follows. An appropriate amount of the phospholipids (POPC, POPS) in chloroform were aliquoted into a small glass vessel and dried by N_2 gas, and then the solvent was further removed by placing the sample in a lyophilizer (BenchTopPro with Omnitronics, SP Scientific, Warminster, PA) overnight. 200 μL of HEPES buffer (10 mM HEPES, 100 mM NaCl, pH 7.4) was added to the dry lipid powder and briefly vortexed, followed by extrusion (Avanti Polar Lipids, Inc.) to prepare 1.0 μm (in diameter) vesicles. HIAPP was prepared by initially dissolving the peptide in HFIP at a concentration of 1 mg/mL and aliquoted into eppendorf tubes in the amount of 0.3 mg hIAPP. The peptide was lyophilized overnight and the dried powder was dissolved in 2 μL dimethyl sulfoxide (DMSO), 2 μL of 100 nM HCl, and diluted in HEPES buffer to a total volume of 50 μL. This peptide stock solution was then added to LUVs to a final concentration of 1 or 3 mol% peptide to lipids.

2.8. ^{31}P solid-state NMR

All of the experiments were performed on an Agilent/Varian 500 MHz solid-state NMR spectrometer operating at the resonance frequency of 500 MHz for ^{1}H and 200 MHz for ^{31}P nuclei. A temperature control unit (Varian) was used to maintain the sample temperature at 37 °C. All ^{31}P spectra were collected using a spin-echo sequence (90°-tau-180°-tau; with tau = 60 μs) under 25 kHz two-pulse phase modulation decoupling (TPPM) of protons. A typical ^{31}P 90 pulse width of 7 μs was used with a recycle delay of 3 s. The ^{31}P chemical shift spectra were referenced with respect to 85% H_3PO_4 at 0 ppm. In each experiment, the ^{31}P control spectrum of 200 μL LUVs, composed of 4 mg of 7:3 POPC/POPS in a 5 mm glass tube, was acquired first (5 mm liquid NMR tubes were cut to fit into a solid-state NMR probe). After collecting the control spectrum, 20 μL of hIAPP was added into the same sample tube to make the final peptide:lipid molar ratio of 1:100 or 3:100. For each sample, seven sequential experiments were then set to collect ^{31}P NMR spectra with each acquisition totaling ~50 min (1000 scans and 3 s recycle delay). POPC/POPS samples were then exposed to 500 μM $MnCl_2$ for the paramagnetic relaxation enhancement (PRE) measurements. All ^{31}P NMR spectra were processed with 300 Hz line broadening using the VnmrJ software.

3. Results and discussion

3.1. ^{31}P NMR reveals hIAPP induces large-scale membrane disruption

HIAPP amyloid growth in water significantly depends on protein concentration [39]. Moreover, as already mentioned, hIAPP induces membrane disruption by two steps: the first step is ascribable to pore

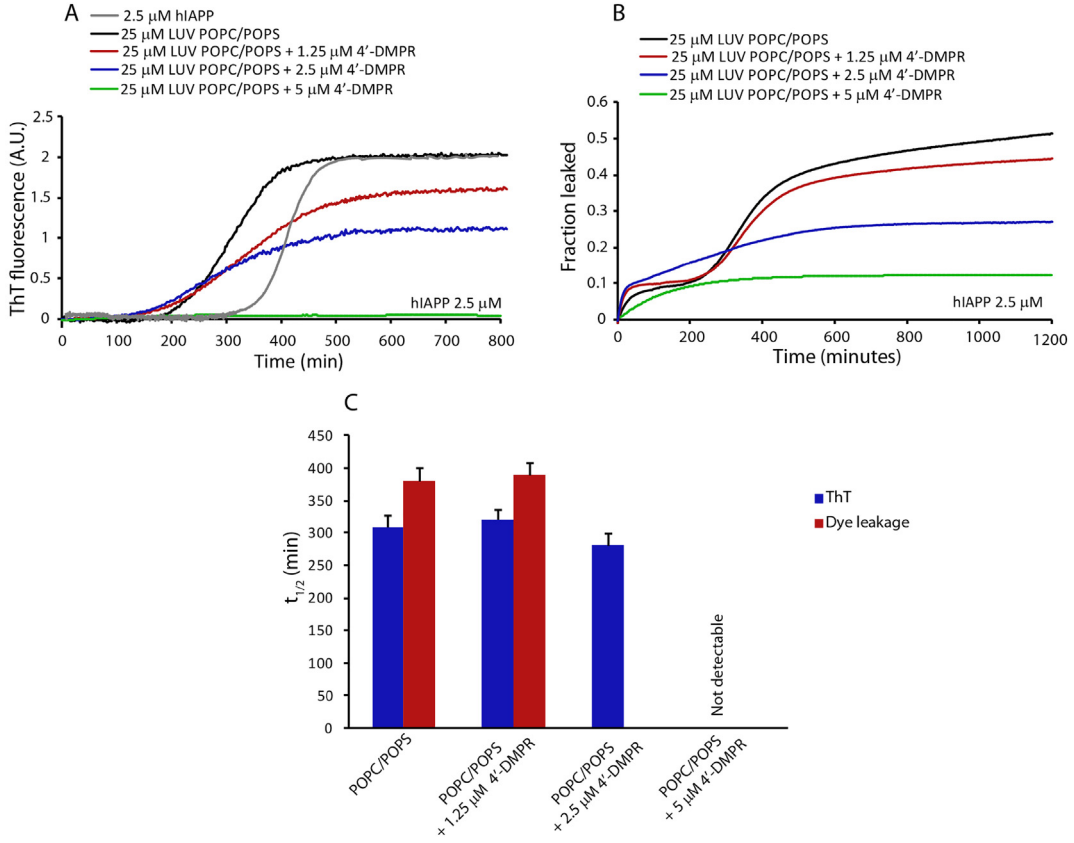

Fig. 6. A) ThT fluorescence traces of hIAPP fiber growth in the presence of 7:3 POPC/POPS LUVs and increasing amounts of 4′-DMPR. All measurements were performed in 10 mM phosphate buffer, 100 mM NaCl, pH 7.4, at 25 °C. Fiber growth kinetics of lipid-free hIAPP is also reported for comparison (grey curve). The traces shown are the average of 3 independent experiments. B) Effect of 4′-DMPR on the mechanism of 7:3 POPC/POPS LUV disruption induced by hIAPP measured by dye leakage assay. All measurements were performed in 10 mM phosphate buffer, 100 mM NaCl, pH 7.4, at 25 °C. The traces shown are the average of 3 independent experiments. C) Comparison of $t_{1/2}$ of fiber formation and membrane damage processes (see also Table 1).

formation mainly due to membrane binding of hIAPP monomers and/or small oligomers. To gain further insight into the mechanism of membrane disruption by hIAPP, we first employ ^{31}P NMR experiments to test the effect of hIAPP concentration over pore formation using ^{31}P NMR and Mn^{2+} as a probe for membrane leakage. Mn^{2+} ions are a convenient probe for this study since they may detect also small pores and quench the ^{31} P NMR signal by shortening the T_2 relaxation time.

A series of static ^{31}P NMR spectra were acquired on 7:3 POPC/POPS LUVs in the absence and presence of 1 mol% or 3 mol% hIAPP to monitor membrane perturbations over the time course of hIAPP aggregation (Fig. 2). All spectra show a chemical shift powder pattern with a span of ~40 ppm, as expected for unilamellar lipid bilayers of liquid crystalline phase. Interestingly, none of the spectra exhibit an observable isotropic peak near 0 ppm. This observation indicates that hIAPP-induced membrane disruption did not produce small fragments of lipid vesicles that can tumble fast enough to be observed on the NMR timescale. Such fragmentation has been observed for antimicrobial peptides [40] and also for amyloid-beta [37,41]. On the other hand, it may be possible that hIAPP induced fragmentations of lipids from the bilayer are immobile in the NMR time scale as they could be incorporated within hIAPP amyloid fibers. Another possibility is that the incubation time was insufficient to observe the detergent-type lipid bilayer fragmentation by hIAPP under the experimental conditions used in the NMR experiments.

Although no isotropic peak near 0 ppm was observed in ^{31}P NMR spectra, paramagnetic relaxation enhancement (PRE) experiments suggest hIAPP induces membrane disruption, consistent with dye leakage experiments. Paramagnetic Mn^{2+} ions in the solvent can reveal if a lipid headgroup is exposed to solvent by inducing broadening of the ^{31}P resonance. Thus, if a lipid bilayer is intact, only the outer leaflet lipids are exposed to the PRE effect from Mn^{2+} ions, which result in broadening of ^{31}P NMR signals arising from outer leaflet lipids. Conversely, if any membrane disruption occurs (by pores or fragmentation), ^{31}P line-broadening will be detected from the exposure of inner leaflet lipids to paramagnetic Mn^{2+} ions in addition to outer leaflet lipids. Fig. 3 shows the effect of Mn^{2+} ions on POPC/POPS LUVs after 10 h of incubation with hIAPP. Phosphorus-31 NMR spectra of LUVs without and with 1 mol% hIAPP (Fig. 3A and B) exhibit much < 50% reduction in the ^{31}P NMR signal intensity suggesting only the lipids in the outer leaflet are affected by the PRE effect and therefore there is little to no membrane permeation of Mn^{2+} ions across the lipid bilayer. However, at 3 mol% hIAPP (Fig. 3C), half of the calculated ^{31}P NMR signal is broadened beyond detection, indicating that paramagnetic Mn^{2+} ions most likely permeated the membrane to quench ^{31}P resonances from the inner leaflet lipids in addition to those in the outer leaflet of the lipid bilayer. HIAPP has been shown to cause membrane disruption by both pore formation and membrane fragmentation. Static ^{31}P NMR experiments presented in this study clearly demonstrate membrane disruption by hIAPP is occurring. The absence of small-size lipid fragments induced by the peptide aggregation at the membrane surface may be attributed to the presence of large-size lipid fragments from the membrane that are unobservable on the NMR timescale, which is unlikely. Instead, if the large-size lipid fragments changed the phase to gel state, the ^{31}P line width gets wider and featureless to cause the signal loss effect. This is further confirmed from solid-state NMR experiments on LUVs containing a PE lipid that is known to promote membrane fragmentation by hIAPP [19].

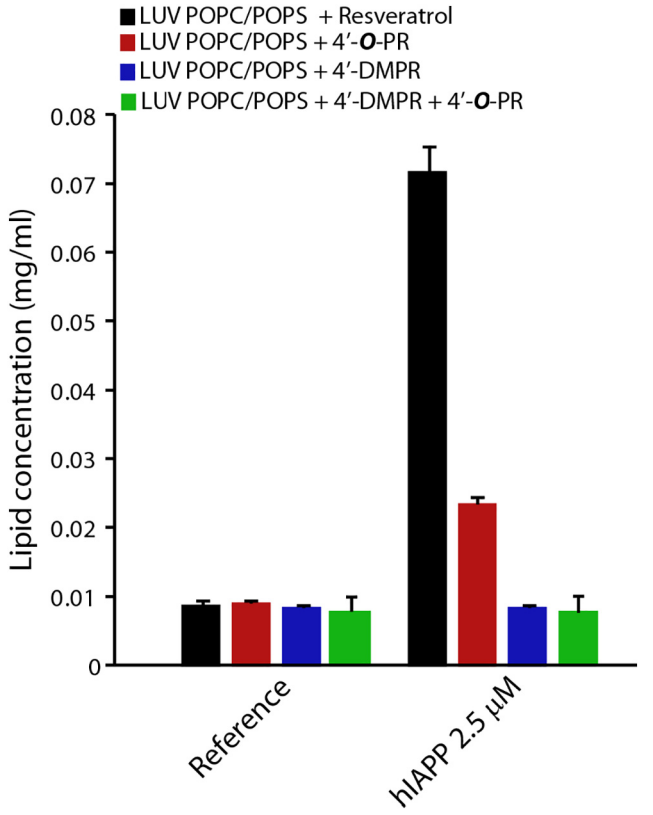

Fig. 7. Stewart assay performed after 24 h of incubation of 7:3 POPC/POPS LUVs with hIAPP. The presence of 4′-DMPR completely inhibits micelle-like structure formation, evidencing that detergent-like mechanism cannot occur.

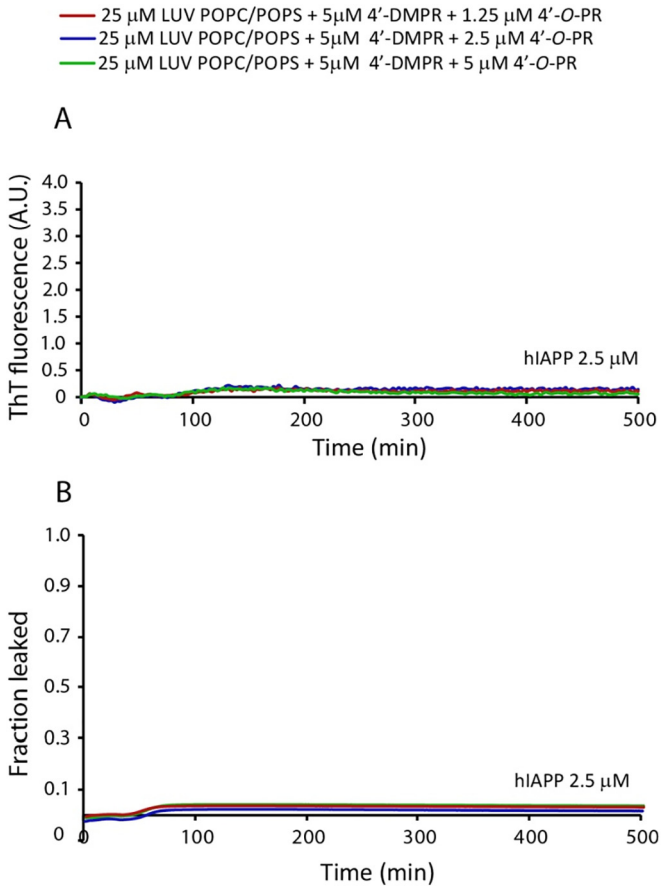

Fig. 8. A) Combined effect of 4′-DMPR and 4′-*O*-PR on hIAPP fiber formation kinetics in the presence of 7:3 POPC/POPS LUVs measured by ThT assay. All measurements were performed in 10 mM phosphate buffer, 100 mM NaCl, pH 7.4, at 25 °C. B) combined effect of 4′-DMPR and 4′-*O*-PR on the mechanism of 7:3 POPC/POPS LUV disruption induced by hIAPP measured by dye leakage assay. All measurements were performed in 10 mM phosphate buffer, 100 mM NaCl, pH 7.4, at 25 °C.

3.2. Effects of resveratrol on hIAPP fiber growth kinetics and membrane disruption

The ability of resveratrol to prevent hIAPP fiber formation in water solution is largely documented [29,42]. However, limited information is available in the presence of lipid membranes. Thus, we first addressed the effect of resveratrol on hIAPP fiber formation kinetics in the presence of 7:3 POPC/POPS LUVs by ThT fluorescence assays. We remind that lipid vesicles with a similar composition are often chosen as the most representative model of β-cells lipid membranes [43]. Resveratrol (1.25 to 5 μM) has exhibited only a poor effect on amyloid growth kinetics (Fig. 4A). Next, to probe its effect on hIAPP-induced membrane disruption, we performed parallel dye leakage assays (Fig. 4B). A comparison of ThT and dye-leakage assays suggests that resveratrol can inhibit amyloid pore formation [19], whereas it is not able to prevent the second step of membrane disruption, correlated with the elongation of the fiber on the membrane surface. These results support the hypothesis that if, on one hand resveratrol does not interfere with membrane-catalyzed hIAPP fiber growth [44,45], still it partly inhibits the first step of membrane disruption (via poration) [46–48], which normally occurs within the first 100 min. However, aggregation of membrane-bound hIAPP is not affected by resveratrol and is causative of membrane damage through a detergent-like mechanism [19,37,38]. Remarkably, resveratrol enhances the rate of the second step of membrane damage, likely due to the presence of a larger number of membrane-active protofibrils.

3.3. Effect of 4′-O-PR on hIAPP fiber formation and membrane damage

Due to poor water solubility, it is likely that, in many ThT assays, the actual level of resveratrol is much lower than its analytical concentration. Indeed, it has been shown that, as other polyphenols, resveratrol may self-assemble in aqueous solution giving rise to large aggregates [45]. Since IAPP-resveratrol interactions are stabilized by hydrogen bonds and π-π stacking combined with hydrophobic interactions, large resveratrol aggregates are expected to exhibit a low affinity for the polypeptide. As a possible strategy to overcome these drawbacks, we synthesized the phosphorylresveratrol derivative 4′-*O*-PR (Fig. 1). Indeed, conjugation by a phosphoryl group has already demonstrated to improve water solubility of resveratrol [33]. However, we don't know how conjugation by a phosphoryl group affects the pharmacological properties of the parent compound. In order to qualitatively answer to this concern, we calculated, for both resveratrol and 4′-*O*-PR, the molecular descriptors based on the Lipinski's 'rule of 5' (Ro5), a widely accepted general guideline to determine if a chemical compound has molecular properties that are compatible to a pharmacological application [49–51]. In particular, Log P (octanol/water partition coefficient) is a measure of the hydrophobicity of the molecule; Molecular Total Polar Surface Area (TPSA) is a good descriptor of drug absorption and blood-brain barrier penetration; the number of rotatable bonds (nrotb) is related to molecular flexibility and it has been shown to be a very good descriptor of oral bioavailability of drugs. Rotatable bonds are defined as any single non-ring bond that is bounded to a non-terminal heavy (i.e., non-hydrogen) atom. Molecular properties of resveratrol and 4′-*O*-PR were calculated by the web based tool Molinspiration. The results reported in Table 2 give evidence that conjugation of resveratrol to the phosphoryl moiety has improved the molecular properties of the parent molecule in terms of bioavailability

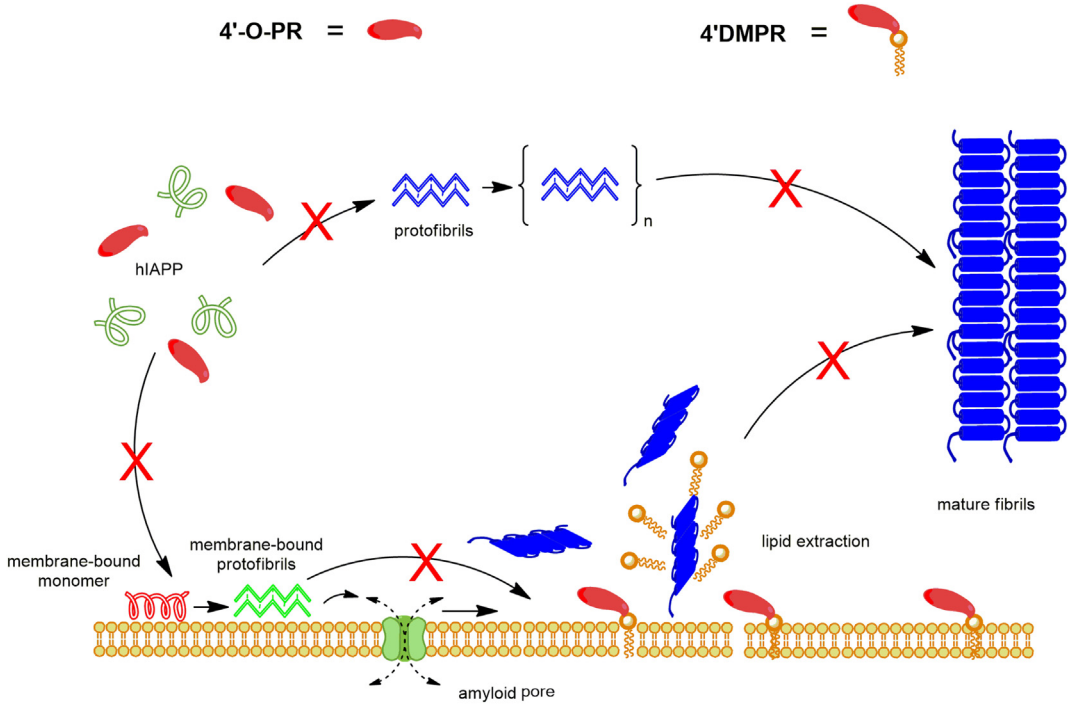

Fig. 9. Schematic representation of the effect of 4′-DMPR and 4′-*O*-PR on hIAPP amyloid formation and membrane disruption. Misfolding of soluble hIAPP monomers initiates aggregation processes involving the formation of β-sheet rich oligomers and eventually, amyloid fibrils. In the water phase, the presence of 4′-*O*-PR inhibits amyloid growth and fibril formation. hIAPP monomers may also bind to lipid membrane surfaces where they acquire an α-helix structure. Next, gathering of hIAPP proteins on the membrane surface induces their assembling into β sheet-rich aggregates. When proteins arrive at a threshold concentration, they assemble to form a pore thus enabling the release of membrane contents. Concurrent with this mechanism, ring-like hIAPP protofibrils may assemble in solution and permeabilize the membrane. Moreover, hIAPP amyloid aggregates may grow at the membrane surface and induce lipid extraction and membrane thinning in a detergent-like mechanism. All these adverse events occurring at the membrane surfaces are inhibited by the presence of 4′-DMPR.

and adsorption.

Therefore, we assayed the anti-aggregating effect of the soluble compound 4′-*O*-PR. Fig. 5A reports ThT assays of hIAPP performed in the presence of POPC/POPS LUVs and using 4′-*O*-PR as the anti-aggregating agent. Although hIAPP aggregation kinetics are not affected by 4′-*O*-PR, the apparent amount of fibrils formed is significantly decreased in the presence of the resveratrol derivative. Parallel dye leakage assays (Fig. 5B) show a complete inhibition of membrane poration and a reduction of the detergent-like membrane disruption mechanism, in agreement with the observed lower amount of hIAPP fibers formed.

3.4. Effect of 4′-DMPR on the hIAPP amyloid growth kinetics

In order to inhibit the second step of membrane disruption, we employed the lipid resveratrol derivative 4′-DMPR. The idea behind the choice of this derivative is that anchoring resveratrol molecules on the membrane surface should abolish hIAPP amyloid growth on the lipid surface and consequently the second step of membrane damage. We use the DMPC derivative of resveratrol because the thickness of POPC and DMPC bilayers are very similar and phase segregation phenomena are thus avoided [52]. ThT curves of hIAPP fiber formation occurring in POPC/POPS membranes incorporating different amounts of 4′-DMPR are shown in Fig. 6A. As expected, the amount of fibers formed decreases on increasing percentages of 4′-DMPR incorporated within POPC/POPS LUVs and in the presence of 5 μM 4′-DMPR hIAPP fiber growth is completely inhibited. Furthermore, the presence of 4′-DMPR in lipid samples (Fig. 6B) does not prevent the first step of membrane disruption (pore formation process) but rather, inhibits the second step of membrane disruption dose-dependently in accordance with ThT traces. These results suggest that resveratrol moieties anchored to the lipid tail and lying on the membrane surface would prevent membrane disruption by a detergent-like mechanism ascribable to the elongation of the fiber on the membrane. However, pore formation can still occur given that it is more likely due to membrane active small intermediates formed during the amyloid growth process occurring first in the aqueous phase.

To further verify whether the presence of 4′-DMPR inhibits the membrane disruption process induced by the elongation of hIAPP fiber on the lipid surface, we performed an experiment to measure the presence of micelle-like structure in solution after the fiber formation process is completed, as described in Materials and methods section. Results shown in Fig. 7 clearly confirm that the presence of 4′-DMPR completely inhibits lipid extraction linked to a detergent-like mechanism of membrane disruption.

3.5. Effect of 4′-O-PR and 4′-DMPR on both hIAPP amyloid growth and membrane disruption

As we pointed out before, hIAPP-induced membrane disruption is a two step process in which the formation of amyloid pores is accompanied by fiber elongation on the membrane surface [19,37]. In the previous sections, we have evidenced that 4′-*O*-PR and 4′-DMPR can inhibit poration and detergent-like lipid extraction, respectively. Thus, we have tested whether the combined use of these two molecules may protect membranes from both the effects of hIAPP amyloids on lipid surface. In Fig. 8A and B we report ThT and dye leakage assays for samples containing 7:3 POPC/POPS LUVs with a 20% (5 μM) of the compound 4′-DMPR and three different concentrations of 4′-*O*-PR. All the experiments confirmed the complete inhibition of both fiber formation and membrane damage.

4. Conclusions

An increasingly large body of evidence indicates that hIAPP toxicity may be related to its abnormal interactions with the cell membrane. In particular, small-sized proto-fibrils were shown to have a higher propensity to permeabilize the membrane when compared to monomeric or fully fibrillar hIAPP. Moreover, microscopic images of pore-like membrane-bound hIAPP oligomers show evident morphological similarities with membrane-leaking structures of toxins, which are known to form pore structures on cell membranes. Nevertheless, poration may represent only a part of the membrane disruption process and other effects including lipid extraction into growing hIAPP amyloid fibrils are also believed to play an important role. This complex mechanism of membrane destabilization implies that simply inhibiting hIAPP amyloid growth might not be sufficient to protect cells. In the present study, we demonstrate that the incorporation of a lipid-anchored resveratrol derivative named 4′-DMPR within a POPC/POPS model membrane may protect the lipid bilayer from a hIAPP-induced lipid extraction through a detergent-like mechanism but not from poration induced by small oligomers. Conversely, a water-soluble resveratrol derivative, 4′-*O*-PR, protects the model membrane from poration phenomena but cannot inhibit lipid extraction occurring through membrane-bound hIAPP amyloid growth. When 4′-*O*-PR is added to the water phase of a lipid dispersion of POPC/POPS LUVs, which also incorporates 4′-DMPR, neither fibril growth nor membrane destabilization are observed (see Fig. 9). Conclusively, results presented in this work suggest a novel strategy to inhibit both the two steps of hIAPP-induced membrane damage i.e. poration and lipid extraction by amyloid fibrils.

Transparency document

The Transparency document associated with this article can be found, in online version.

Acknowledgements

This work was financially supported by the Italian MiUR program PRIN 20157WZM8A and National Institute of Health (AG048934 to A.R.).

References

[1] W.H. Herman, P. Zimmet, Type 2 diabetes: an epidemic requiring global attention and urgent action, Diabetes Care 35 (2012) 943–944.
[2] L.M. Jaacks, K.R. Siegel, U.P. Gujral, K.M.V. Narayan, Type 2 diabetes: a 21st century epidemic, Best Pract. Res. Clin. Endocrinol. Metab. 30 (2016) 331–343.
[3] S.A. Tabish, Is diabetes becoming the biggest epidemic of the twenty-first century? Int. J. Health Sci. 1 (2007) V–VIII.
[4] A. Mukherjee, D. Morales-Scheihing, P.C. Butler, C. Soto, Type 2 diabetes as a protein misfolding disease, Trends Mol. Med. 21 (2015) 439–449.
[5] G.J. Cooper, A.C. Willis, A. Clark, R.C. Turner, R.B. Sim, K.B. Reid, Purification and characterization of a peptide from amyloid-rich pancreases of type 2 diabetic patients, Proc. Natl. Acad. Sci. U. S. A. 84 (1987) 8628–8632.
[6] P. Westermark, C. Wernstedt, T.D. O'Brien, D.W. Hayden, K.H. Johnson, Islet amyloid in type 2 human diabetes mellitus and adult diabetic cats contains a novel putative polypeptide hormone, Am. J. Pathol. 127 (1987) 414–417.
[7] P. Westermark, C. Wernstedt, E. Wilander, K. Sletten, A novel peptide in the calcitonin gene related peptide family as an amyloid fibril protein in the endocrine pancreas, Biochem. Biophys. Res. Commun. 140 (1986) 827–831.
[8] J. Janson, R.H. Ashley, D. Harrison, S. McIntyre, P.C. Butler, The mechanism of islet amyloid polypeptide toxicity is membrane disruption by intermediate-sized toxic amyloid particles, Diabetes 48 (1999) 491–498.
[9] D. Milardi, M.F.M. Sciacca, M. Pappalardo, D.M. Grasso, C. La Rosa, The role of aromatic side-chains in amyloid growth and membrane interaction of the islet amyloid polypeptide fragment LANFLVH, Eur. Biophys. J. 40 (2011) 1–12.
[10] M.F.M. Sciacca, M. Pappalardo, F. Attanasio, D. Milardi, C.L. Rosa, D.M. Grasso, Are fibril growth and membrane damage linked processes? An experimental and computational study of IAPP 12–18 and IAPP 21–27 peptides, New J. Chem. 34 (2010) 200–207.
[11] H.A. Lashuel, D. Hartley, B.M. Petre, T. Walz, P.T. Lansbury Jr., Neurodegenerative disease: amyloid pores from pathogenic mutations, Nature 418 (2002) 291, http://dx.doi.org/10.1038/418291a.
[12] T.A. Mirzabekov, M.C. Lin, B.L. Kagan, Pore formation by the cytotoxic islet amyloid peptide amylin, J. Biol. Chem. 271 (1996) 1988–1992.
[13] Y. Porat, S. Kolusheva, R. Jelinek, E. Gazit, The human islet amyloid polypeptide forms transient membrane-active prefibrillar assemblies, Biochemistry (Mosc) 42 (2003) 10971–10977.
[14] M. Pannuzzo, A. Raudino, D. Milardi, C.L. Rosa, M. Karttunen, α-Helical structures drive early stages of self-assembly of amyloidogenic amyloid polypeptide aggregate formation in membranes, Sci. Rep. 3 (2013) 2781.
[15] S. Scalisi, M.F.M. Sciacca, G. Zhavnerko, D.M. Grasso, G. Marletta, C. La Rosa, Self-assembling pathway of HiApp fibrils within lipid bilayers, Chembiochem Eur. J. Chem. Biol. 11 (2010) 1856–1859.
[16] F. Lolicato, A. Raudino, D. Milardi, C. La Rosa, Resveratrol interferes with the aggregation of membrane-bound human-IAPP: a molecular dynamics study, Eur. J. Med. Chem. 92 (2015) 876–881.
[17] M.F.M. Sciacca, F. Lolicato, G. Di Mauro, D. Milardi, L. D'Urso, C. Satriano, A. Ramamoorthy, C. La Rosa, The role of cholesterol in driving IAPP-membrane interactions, Biophys. J. 111 (2016) 140–151.
[18] M.F.M. Engel, L. Khemtémourian, C.C. Kleijer, H.J.D. Meeldijk, J. Jacobs, A.J. Verkleij, B. de Kruijff, J.A. Killian, J.W.M. Höppener, Membrane damage by human islet amyloid polypeptide through fibril growth at the membrane, Proc. Natl. Acad. Sci. U. S. A. 105 (2008) 6033–6038.
[19] M.F.M. Sciacca, J.R. Brender, D.-K. Lee, A. Ramamoorthy, Phosphatidylethanolamine enhances amyloid fiber-dependent membrane fragmentation, Biochemistry (Mosc) 51 (2012) 7676–7684.
[20] J.R. Brender, E.L. Lee, K. Hartman, P.T. Wong, A. Ramamoorthy, D.G. Steel, A. Gafni, Biphasic effects of insulin on islet amyloid polypeptide membrane disruption, Biophys. J. 100 (2011) 685–692.
[21] F. Yang, G.P. Lim, A.N. Begum, O.J. Ubeda, M.R. Simmons, S.S. Ambegaokar, P.P. Chen, R. Kayed, C.G. Glabe, S.A. Frautschy, G.M. Cole, Curcumin inhibits formation of amyloid beta oligomers and fibrils, binds plaques, and reduces amyloid in vivo, J. Biol. Chem. 280 (2005) 5892–5901.
[22] M.F.M. Sciacca, V. Romanucci, A. Zarrelli, I. Monaco, F. Lolicato, N. Spinella, C. Galati, G. Grasso, L. D'Urso, M. Romeo, L. Diomede, M. Salmona, C. Bongiorno, G. Di Fabio, C. La Rosa, D. Milardi, Inhibition of Aβ amyloid growth and toxicity by Silybins: the crucial role of stereochemistry, ACS Chem. Neurosci. 8 (2017) 1767–1778.
[23] S.-J. Hyung, A.S. DeToma, J.R. Brender, S. Lee, S. Vivekanandan, A. Kochi, J.-S. Choi, A. Ramamoorthy, B.T. Ruotolo, M.H. Lim, Insights into antiamyloidogenic properties of the green tea extract (−)-epigallocatechin-3-gallate toward metal-associated amyloid-β species, Proc. Natl. Acad. Sci. U. S. A. 110 (2013) 3743–3748.
[24] M. Algamal, R. Ahmed, N. Jafari, B. Ahsan, J. Ortega, G. Melacini, Atomic-resolution map of the interactions between an amyloid inhibitor protein and amyloid beta (Aβ) peptides in the monomer and protofibril states, J. Biol. Chem. 292 (42) (2017) 17158–17168.
[25] M. Algamal, J. Milojevic, N. Jafari, W. Zhang, G. Melacini, Mapping the interactions between the Alzheimer's Aβ-peptide and human serum albumin beyond domain resolution, Biophys. J. 105 (2013) 1700–1709.
[26] R. Ahmed, B. VanSchouwen, N. Jafari, X. Ni, J. Ortega, G. Melacini, Molecular mechanism for the (−)-epigallocatechin gallate-induced toxic to nontoxic remodeling of Aβ oligomers, J. Am. Chem. Soc. 139 (2017) 13720–13734.
[27] C. Lu, Y. Guo, J. Yan, Z. Luo, H.-B. Luo, M. Yan, L. Huang, X. Li, Design, synthesis, and evaluation of multitarget-directed resveratrol derivatives for the treatment of Alzheimer's disease, J. Med. Chem. 56 (2013) 5843–5859.
[28] A. Pithadia, J.R. Brender, C.A. Fierke, A. Ramamoorthy, Inhibition of IAPP aggregation and toxicity by natural products and derivatives, J. Diabetes Res. 2016 (2016).
[29] R. Mishra, D. Sellin, D. Radovan, A. Gohlke, R. Winter, Inhibiting islet amyloid polypeptide fibril formation by the red wine compound resveratrol, Chembiochem 10 (2009) 445–449.
[30] Q. Wang, L. Ning, Y. Niu, H. Liu, X. Yao, Molecular mechanism of the inhibition and remodeling of human islet amyloid polypeptide (hIAPP1–37) oligomer by resveratrol from molecular dynamics simulation, J. Phys. Chem. B 119 (2015) 15–24.
[31] A. Amri, J.C. Chaumeil, S. Sfar, C. Charrueau, Administration of resveratrol: what formulation solutions to bioavailability limitations? J. Control. Release 158 (2012) 182–193.
[32] J. Gambini, M. Inglés, G. Olaso, R. Lopez-Grueso, V. Bonet-Costa, L. Gimeno-Mallench, C. Mas-Bargues, K.M. Abdelaziz, M.C. Gomez-Cabrera, J. Vina, C. Borras, Properties of resveratrol: in vitro and in vivo studies about metabolism, bioavailability, and biological effects in animal models and humans, Oxidative Med. Cell. Longev. 2015 (2015).
[33] D. Aleo, V. Cardile, R. Chillemi, G. Granata, S. Sciuto, Chemoenzymatic synthesis and some biological properties of O-phosphoryl derivatives of (E)-resveratrol, Nat. Prod. Commun. 3 (2008) 1693–1700.
[34] R. Chillemi, N. Cardullo, V. Greco, G. Malfa, B. Tomasello, S. Sciuto, Synthesis of amphiphilic resveratrol lipoconjugates and evaluation of their anticancer activity towards neuroblastoma SH-SY5Y cell line, Eur. J. Med. Chem. 96 (2015) 467–481.
[35] R.C. MacDonald, R.I. MacDonald, B.P.M. Menco, K. Takeshita, N.K. Subbarao, L. Hu, Small-volume extrusion apparatus for preparation of large, unilamellar vesicles, Biochim. Biophys. Acta Biomembr. 1061 (1991) 297–303.
[36] J.C. Stewart, Colorimetric determination of phospholipids with ammonium ferrothiocyanate, Anal. Biochem. 104 (1980) 10–14.
[37] M.F.M. Sciacca, S.A. Kotler, J.R. Brender, J. Chen, D. Lee, A. Ramamoorthy, Two-step mechanism of membrane disruption by Aβ through membrane fragmentation and pore formation, Biophys. J. 103 (2012) 702–710.
[38] M.F. Sciacca, D. Milardi, G.M. Messina, G. Marletta, J.R. Brender, A. Ramamoorthy, C. La Rosa, Cations as switches of amyloid-mediated membrane disruption mechanisms: calcium and IAPP, Biophys. J. 104 (2013) 173–184.

[39] J.R. Brender, J. Krishnamoorthy, M.F.M. Sciacca, S. Vivekanandan, L. D'Urso, J. Chen, C. La Rosa, A. Ramamoorthy, Probing the sources of the apparent irreproducibility of amyloid formation: drastic changes in kinetics and a switch in mechanism due to micellelike oligomer formation at critical concentrations of IAPP, J. Phys. Chem. B 119 (2015) 2886–2896.
[40] D.-K. Lee, J.R. Brender, M.F.M. Sciacca, J. Krishnamoorthy, C. Yu, A. Ramamoorthy, Lipid composition-dependent membrane fragmentation and pore-forming mechanisms of membrane disruption by Pexiganan (MSI-78), Biochemistry (Mosc) 52 (2013).
[41] K.J. Korshavn, C. Satriano, Y. Lin, R. Zhang, M. Dulchavsky, A. Bhunia, M.I. Ivanova, Y.-H. Lee, C.L. Rosa, M.H. Lim, A. Ramamoorthy, Reduced lipid bilayer thickness regulates the aggregation and cytotoxicity of amyloid-β, J. Biol. Chem. 292 (2017) 4638–4650.
[42] L.-H. Tu, L.M. Young, A.G. Wong, A.E. Ashcroft, S.E. Radford, D.P. Raleigh, Mutational analysis of the ability of resveratrol to inhibit amyloid formation by islet amyloid polypeptide: critical evaluation of the importance of aromatic–inhibitor and histidine–inhibitor interactions, Biochemistry 54 (2015) 666–676.
[43] I. Rustenbeck, A. Matthies, S. Lenzen, Lipid composition of glucose-stimulated pancreatic islets and insulin-secreting tumor cells, Lipids 29 (1994) 685–692.
[44] P. Jiang, W. Li, J.-E. Shea, Y. Mu, Resveratrol inhibits the formation of multiple-layered β-sheet oligomers of the human islet amyloid polypeptide segment 22–27, Biophys. J. 100 (2011) 1550–1558.
[45] P. Nedumpully-Govindan, A. Kakinen, E.H. Pilkington, T.P. Davis, P. Chun Ke, F. Ding, Stabilizing off-pathway oligomers by polyphenol nanoassemblies for IAPP aggregation inhibition, Sci. Rep. 6 (2016) 19463.
[46] M. Zhang, B. Ren, Y. Liu, G. Liang, Y. Sun, L. Xu, J. Zheng, Membrane interactions of hIAPP monomer and oligomer with lipid membranes by molecular dynamics simulations, ACS Chem. Neurosci. 8 (2017) 1789–1800.
[47] N. Bag, A. Ali, V.S. Chauhan, T. Wohland, A. Mishra, Membrane destabilization by monomeric hIAPP observed by imaging fluorescence correlation spectroscopy, Chem. Commun. (Camb.) 49 (2013) 9155–9157.
[48] M.F.M. Engel, H. Yigittop, R.C. Elgersma, D.T.S. Rijkers, R.M.J. Liskamp, B. de Kruijff, J.W.M. Höppener, J. Antoinette Killian, Islet amyloid polypeptide inserts into phospholipid monolayers as monomer, J. Mol. Biol. 356 (2006) 783–789, http://dx.doi.org/10.1016/j.jmb.2005.12.020.
[49] P. Ertl, B. Rohde, P. Selzer, Fast calculation of molecular polar surface area as a sum of fragment-based contributions and its application to the prediction of drug transport properties, J. Med. Chem. 43 (2000) 3714–3717.
[50] C.A. Lipinski, F. Lombardo, B.W. Dominy, P.J. Feeney, Experimental and computational approaches to estimate solubility and permeability in drug discovery and development settings, Adv. Drug Deliv. Rev. 46 (2001) 3–26.
[51] D.F. Veber, S.R. Johnson, H.-Y. Cheng, B.R. Smith, K.W. Ward, K.D. Kopple, Molecular properties that influence the oral bioavailability of drug candidates, J. Med. Chem. 45 (2002) 2615–2623.
[52] N. Kučerka, M.-P. Nieh, J. Katsaras, Fluid phase lipid areas and bilayer thicknesses of commonly used phosphatidylcholines as a function of temperature, Biochim. Biphys. Acta, Biomembr. 1808 (2011) 2761–2771.